

Insect Inspired Three Dimensional Centring

Luke Cole^{1,2}, Nick Barnes²

December 5, 2008

¹Australian National University
ACT 0200, Australia

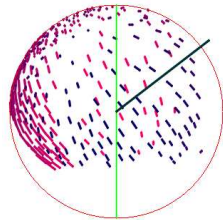
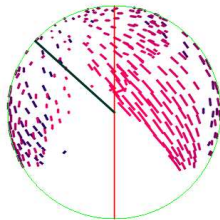
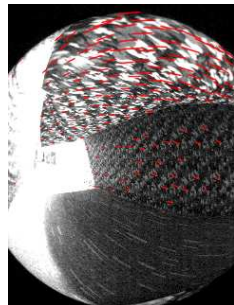
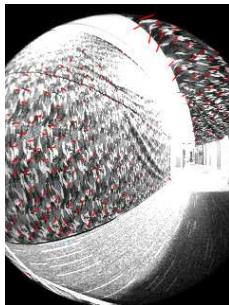
²National ICT Australia,
Locked Bag 8001,
Canberra, ACT 2601

Talk Outline

- Quick Overview of 3D centring.
- Approach to 3D centring.
- Experimental Procedure.
- Results.
- Conclusion.
- Future Work.

Quick Overview of 3D Centring

- Extends the classic example of bee-inspired 2D corridor-centring.
- 2D centring (or corridor-centring) balances the optical flow between the left and right surfaces.
- 3D centring extends 2D centring, by balancing the optical flow between the top and bottom surfaces.
- Example application: flying a helicopter through corridor-like environments.



Approach Introduction

- We use a robotic system that has 4DOF for the vision system. Ideally we choose a robot that doesn't fly - due to the development cost.
- We extend the classical 2D centring to control the vertical motion of the vision system based on the flow in the top and bottom hemispheres.
- Flight simulation robots: cable-array robots, gantry systems, blimps and the InsectBot.

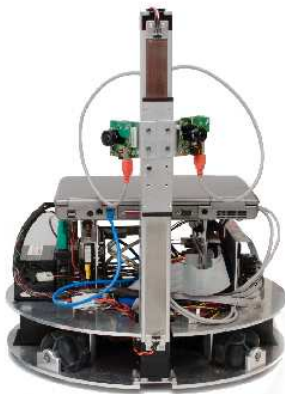


Figure: The InsectBot - 4DOF flight simulator

The InsectBot - A flight simulation robot

- 4DOF vision system - three in the horizontal plane and one in the vertical plane.
- Horizontal motion performed using four omni-directional wheels.
- Vertical motion performed using a custom lift-platform mechanism.
- Needs roll and pitch for true flight simulation.

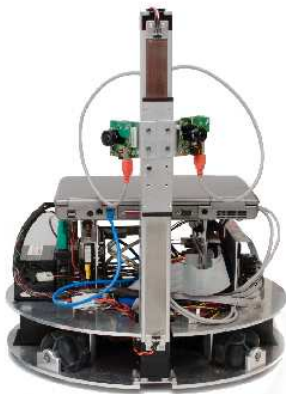


Figure: The InsectBot - 4DOF flight simulator

The Algorithm

- 2D heading direction: $\theta_h = K_h(\tau_l - \tau_r)$
- 3D heading direction, introduces: $\theta_v = K_v(\tau_t - \tau_r)$
- Instead of using the entire hemisphere we use:

$$\tau_l = \frac{\sum_{i=1}^{N_l} (\|\vec{f}_i\| \|\sin(\theta_i)\|)}{N_l}, \tau_r = \frac{\sum_{i=1}^{N_r} (\|\vec{f}_i\| \|\sin(\theta_i)\|)}{N_r} \quad (1)$$

$$\tau_t = \frac{\sum_{i=1}^{N_t} (\|\vec{f}_i\| \|\cos(\theta_i)\|)}{N_t}, \tau_b = \frac{\sum_{i=1}^{N_b} (\|\vec{f}_i\| \|\cos(\theta_i)\|)}{N_b} \quad (2)$$

Experimental Procedure

- Performed in a corridor-like environment.
- Lined the walls and false ceiling with textured material to ensure optical flow could be measured.
- Performed three sets of trials: 2D, 3D, and 3D again but using Equations 1 and 2.
- Each set of trials include four runs. Where each run will start at either the left, or right of the entrance.



Figure: The environment for experimental trials. Left: Entrance. Right: Exit

Videos

2D Results

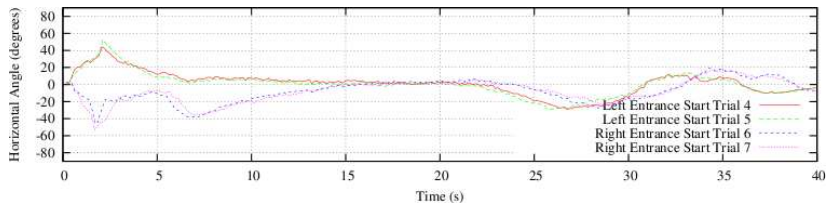


Figure: θ_h for trials without ceiling.

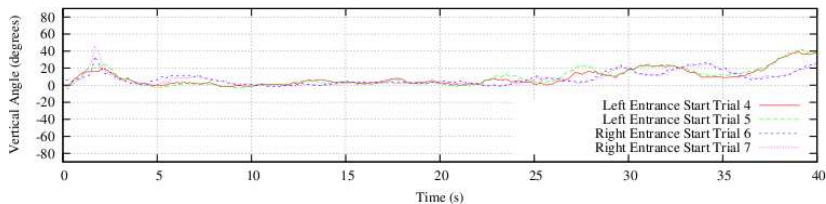


Figure: θ_v for trials without ceiling.

3D Results (Using Equations 1 and 2)

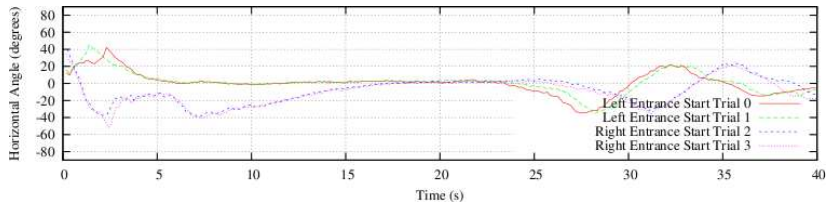


Figure: θ_h for trials with declining ceiling.

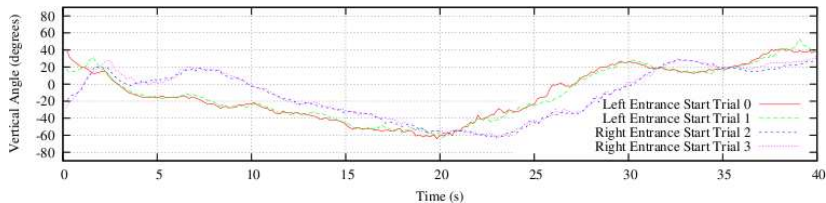


Figure: θ_v for trials with declining ceiling.

3D Results

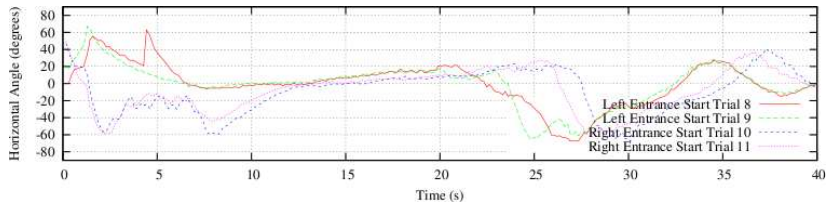


Figure: θ_h for trials with declining ceiling.

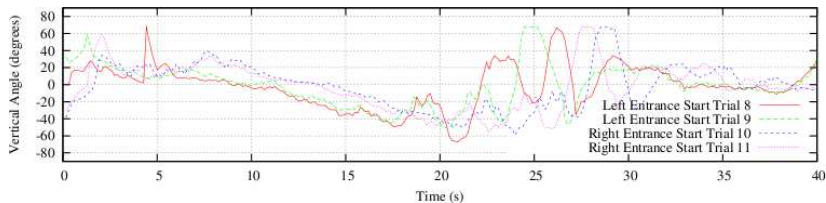


Figure: θ_v for trials with declining ceiling.

Conclusion

- Produced a accurate and smooth response to the changes in the shape of the textured environment.
- Could be used for flying vehicles, to navigate three-dimensional corridor-like environments.
- Needs to handle roll, pitch and rotations before use of a flying vehicle.

Future Work

- Extend algorithm to handle roll and pitch.
- Extend algorithm to handle rotations.
- Test the algorithm on a flying vehicle.

Acknowledgements

Part of this work was supported by funding from NICTA and ANU. NICTA is funded by the Australian Government as represented by the Department of Broadband, Communications and the Digital Economy and the Australian Research Council through the ICT Centre of Excellence program.